Optimization of Braking Phase Coordinates for Energy-Efficient Operation of Pneumatic Systems

Strizhak M., Rogovyi A., Iglin S.

National Technical University «Kharkiv Polytechnic Institute»

Kharkiv, Ukraine

Abstract. The aim of this study is to optimize the operating mode of a pneumatic system by determining the braking start and end coordinates that minimize the piston speed without the use of damping devices. This approach avoids the discharge of compressed air into the atmosphere and brings the operating conditions closer to an energy-saving mode. The goal is achieved through the implementation of a control algorithm that switches the distributor based on the piston position, allowing for the formation of a defined braking trajectory. The study involved mathematical modeling of the transient processes in the pneumatic system, as well as numerical optimization of the braking coordinates using the Nelder–Mead method and exhaustive search. It was found that the optimal braking start and end coordinates should be located within the last 10–15% of the piston stroke to ensure a final velocity of about 0.03 m/s. The most significant result is the development of a generalized dependency between braking coordinates and cylinder stroke length, enabling the design of energy-efficient pneumatic drive modes without the need for additional experimental research. As a result of the optimization, effective piston braking is achieved without damping devices, reducing compressed air losses and increasing the overall energy efficiency of the pneumatic system.

***Keywords*:** pneumatic drive, braking, commutation, energy efficiency, transient process.

Optimizarea coordonatelor fazei de frânare pentru funcționarea eficientă energetic a sistemelor pneumatice
Strijak M., Rogovâi A., Iglin S.
Universitatea Tehnică Națională «Institutul Politehnic Harkov», Harkov, Ucraina

Rezumat. Scopul cercetării este optimizarea regimului de funcționare al sistemului pneumatic prin determinarea coordonatelor de început și sfârșit ale frânării, care asigură reducerea vitezei pistonului până la o valoare minimă, fără utilizarea dispozitivelor de amortizare. Această abordare permite evitarea evacuării aerului comprimat în atmosferă și apropie condițiile de lucru de un regim de economisire a energiei. Realizarea obiectivului propus se realizează prin implementarea unui algoritm de control al comutării distribuitorului, în funcție de poziția pistonului, ceea ce permite formarea unei traiectorii de frânare prestabilite. În cadrul studiului a fost realizată modelarea matematică a proceselor tranzitorii în sistemul pneumatic, precum și optimizarea numerică a coordonatelor de frânare utilizând metodele Nelder-Mead și căutarea exhaustivă. S-a constatat că coordonatele optime ale începutului și sfârșitului frânării trebuie să se afle în ultimele 10–15% din cursa pistonului, pentru a asigura o viteză finală de aproximativ 0,03 m/s. Cel mai important rezultat constă în elaborarea unei dependențe generalizate între coordonatele de frânare și lungimea cursei cilindrului, ceea ce permite proiectarea regimurilor de funcționare eficiente energetic ale acționărilor pneumatice fără cercetări suplimentare. Ca urmare a optimizării, se obține o frânare eficientă a pistonului fără a fi necesară utilizarea dispozitivelor de amortizare, ceea ce reduce pierderile de energie a aerului comprimat și crește eficiența energetică generală a sistemului pneumatic.

***Cuvinte-cheie*:** acționare pneumatică, frânare, comutație, eficiență energetică, proces tranzitoriu.

Оптимизация фазовых координат торможения для энергоэффективной работы пневматических систем
Стрижак М.Г., Роговой А.С., Иглин С.П.
Национальный технический университет «Харьковский политехнический институт», Харьков, Украина

Аннотация. Целью исследования является оптимизация режима работы пневматической системы путем определения координат начала и завершения торможения, обеспечивающих снижение скорости поршня до минимального значения без использования демпфирующих устройств. Такой подход позволяет избежать сброса сжатого воздуха в атмосферу и приблизить условия работы к энергосберегающему режиму. Достижение поставленной цели реализуется за счёт внедрения алгоритма управления переключением распределителя в зависимости от координаты поршня, что позволяет формировать заданную траекторию торможения. В ходе исследования проведено математическое моделирование

переходных процессов в пневмосистеме, реализована численная оптимизация координат торможения методами Нелдера-Мида и полного перебора. Установлено, что оптимальные координаты начала и завершения торможения должны находиться в пределах последних 10–15 % длины хода поршня для обеспечения конечной скорости на уровне 0,03 м/с. Наиболее значимым результатом является построение обобщённой зависимости координат торможения от длины хода цилиндра, что позволяет проектировать энергосберегающие режимы работы пневмопривода без дополнительных исследований. В результате оптимизации достигается эффективное торможение поршня без необходимости использования демпфирующих устройств, что снижает потери энергии сжатого воздуха и повышает общую энергоэффективность пневмосистемы.

Ключевые слова: пневматический привод, торможение, коммутация, энергоэффективность, переходный процесс.

INTRODUCTION

Pneumatic actuators form the foundation of modern automation systems. Due to their advantages – such as simple design, reliability, availability and low cost of the energy carrier (air) – they are widely used across various industries.

However, despite their efficiency, pneumatic systems exhibit a relatively low coefficient of performance. This is primarily due to significant energy losses during air compression, damping losses when the working element decelerates at the end of its stroke, and other factors. Compressed air is an expensive energy carrier, and the energy consumption of pneumatic actuators is considerable [1]. Therefore, energy conservation remains a pressing issue. Notably, the production of compressed air accounts for approximately 7–10% of industrial energy consumption in the European Union [1–4]. At the same time, studies show that the energy-saving potential for compressed air consumers, particularly pneumatic actuators, can reach up to 40% [5–8], and in some cases even 80% [9].

The main factors behind excessive energy consumption include improperly selected actuator sizes, inefficient operating modes [10], and the presence of compressed air leaks. As such, implementing energy-saving operating modes in pneumatic actuators must begin at the design stage, where careful analysis of system parameters and the integration of modern control methods are essential. Reducing energy consumption is also a key step toward achieving climate goals and improving production efficiency.

RESEARCH OVERVIEW

Modern cost-effective industrial pneumatic systems must offer high responsiveness, which is achieved through rapid piston acceleration and maintaining a high movement speed. At the same time, the working process must be safe, meaning that piston impact on the cylinder cap at the end of the stroke—caused by high velocity—should be avoided. Most often, to decelerate the piston at the end of its stroke, modern pneumatic systems use internal or external damping devices that ensure smooth and reliable deceleration even at high speeds [11].

For example, in study [12], a model of an internal pneumatic damper is presented, along with an experimental investigation of changes in pressure, temperature, and piston speed during deceleration in the cushioning zone. The research setup involves a controllable throttle through which air exits the "pocket" at the end of the stroke. Both the model and experimental results confirm that such deceleration significantly reduces impact loads, ensuring effective piston braking. However, the compressed air used to create the damping effect is vented into the atmosphere through the throttle, leading to unnecessary energy losses—especially under high-frequency cycles or with heavy piston loads.

A similar conclusion can be drawn from work [13], which presents numerical modeling and optimization of throttle valve parameters in the cushioning zone for high-speed cylinders. The optimization process considered hole geometry, valve elasticity, and air characteristics in the exhaust chamber. The results demonstrated reduced pneumatic rebound and improved braking smoothness. However, as in the previous study, the system is based on the principle of venting compressed air to the atmosphere, which negatively impacts energy efficiency.

Thus, the use of damping devices enables smooth and reliable deceleration of cylinders, even at high speeds. However, all pressure accumulated in the braking chamber during deceleration is lost through the throttle as expelled air. Such systems remain energy-intensive, limiting their efficiency in industrial applications from a resource-saving standpoint.

Recent research also emphasizes the importance of design solutions in actuator systems operating with compressed media. In particular, it has been established that rational geometry of internal channels and flow distribution elements can significantly affect the system's flow capacity and pressure losses, thereby enhancing overall energy efficiency [14]. Additionally, changes in the spatial arrangement of key components can positively influence the actuator's output characteristics while minimizing parasitic leaks and pressure losses [15]. These approaches can be incorporated into the design of next-generation pneumatic actuators focused on energy saving.

Various methods for improving energy efficiency during braking are applied in modern pneumatic systems. For instance, in [16], a pneumatic system is investigated that reuses the working capacity of exhaust air. The principle involves collecting air discharged from the cylinder into a special receiver and then using it in subsequent cycles. The authors demonstrated air savings of up to 23%, significantly enhancing actuator energy efficiency without altering the core control architecture. In [17], a scheme is proposed that cuts off air supply upon reaching a specified pressure level. The use of controllable valves allows maintaining pressure in working chambers without additional compressed air supply, particularly during holding phases. This approach enables up to 71% energy savings [17].

The review article [18] offers a classification of methods for reducing energy consumption in pneumatic systems. The authors highlight key architectural solutions, including switching schemes, as crucial for achieving energy savings without significant loss of functionality or precision.

In [9], a novel approach is used that changes the switching configuration between the cylinder chambers. Instead of the traditional venting of compressed air into the atmosphere, it is redirected between chambers to brake the cylinder at the end of the stroke or is recovered back into the network. As a result, up to 87% compressed air savings are achieved [9], making these schemes among the most efficient currently available.

PROBLEM STATEMENT

The study of the influence of pneumatic actuator structure on its transient behavior [19] revealed a number of pneumatic circuit configurations that enable both the fulfillment of transient performance requirements (such as high responsiveness and stable operation) and the implementation of an energy-saving operating mode.

The objective of the study is to optimize the working process of a pneumatic system by modifying the switching configurations between the chambers of the cylinder to achieve compressed air energy savings.

The task is to determine the coordinates of the start and end of piston braking in order to achieve minimal piston velocity at the end of its stroke. This would allow eliminating the use of damping devices and the discharge of compressed air into the atmosphere, thereby enabling an energy-efficient operating mode.

RESEARCH METHODS

As an assumption in constructing the mathematical model, we consider the absence of heat exchange between the gas and the surrounding environment. Study [20] has shown that under rapid pressure changes, the simplification of assuming adiabatic processes does not reduce the accuracy of the mathematical model by more than 5–9%. Similarly, article [21] confirms that such an assumption under fast pressure variation results in a reduction of calculation accuracy by only 1–5%.

Another assumption is that the working medium behaves as an ideal gas, which is justified in [22]. That study demonstrates that the deviation of the real transient process from the ideal gas model under standard operating conditions (pressures up to 1 MPa, temperatures up to 400 K) does not exceed 1%. Article [23] establishes that even under elevated pressures, the error introduced by this assumption remains within 5%.

Taking these assumptions into account, we formulate the heat (energy) balance equations for the open (working and exhaust) gas chambers in the form of expressions for the rate of pressure change in these chambers dp_1/dt and dp_2/dt, the differential form of the Clapeyron–Mendeleev equation of state, which is subsequently expressed in terms of the rate of temperature change in these chambers dT_1/dt and dT_2/dt, and the dynamic equilibrium equation of the piston [24–27].

We also introduce into the mathematical model a mass flow function $\varphi(I)$, that accounts for the pressure ratio between the evacuated and

filled chambers (transition from subcritical to supercritical flow regimes) [28–32]. This enables automated switching between gas flow regimes and allows for sign changes in the mass flow rate across all throttling elements:

$$\varphi\left(\frac{p_1}{p_m}\right) = \begin{cases} \sqrt{\dfrac{2}{k-1}\left[\left(\dfrac{p_1}{p_m}\right)^{\frac{2}{k}} - \left(\dfrac{p_1}{p_m}\right)^{\frac{k+1}{k}}\right]} \\ \text{if} \quad 0,528 \le \dfrac{p_1}{p_m} \le 1; \\ 0,579 \quad \text{if} \quad 0 < \dfrac{p_1}{p_m} < 0,528. \end{cases} \quad (1)$$

$$\begin{cases} \dfrac{dp_1}{dt} = \dfrac{k \cdot f_1^e \sqrt{k \cdot R}}{(x_{01}+x)}\left[(1-Y)\dfrac{p_m\sqrt{T_m}}{F_1}\varphi\left(\dfrac{p_1}{p_m}\right) - \right. \\ \left. -Y\dfrac{p_1\sqrt{T_1}}{F_1}\varphi\left(\dfrac{p_a}{p_1}\right)\right] - \dfrac{k \cdot p_1}{x_{01}+x}\dfrac{dx}{dt}; \\[2mm] \dfrac{dT_1}{dt} = \dfrac{T_1}{p_1}\cdot\dfrac{dp_1}{dt} + \dfrac{T_1}{x_{01}+x}\cdot\dfrac{dx}{dt} - \dfrac{f_1^e\sqrt{k\cdot R}}{F_1\cdot(x_{01}+x)} \cdot \\ \cdot\left[(1-Y)\dfrac{T_1^2\cdot p_m\sqrt{T_m}}{p_1\cdot T_m}\cdot\varphi\left(\dfrac{p_1}{p_m}\right) - \right. \\ \left. -Y\cdot T_1\sqrt{T_1}\cdot\varphi\left(\dfrac{p_m}{p_1}\right)\right]; \\[2mm] \dfrac{dp_2}{dt} = -\dfrac{k\cdot f_2^e\sqrt{k\cdot R}}{L+x_{02}-x}\left\{(1-Y)\dfrac{p_2\sqrt{T_2}}{F_2}\varphi\left(\dfrac{p_a}{p_m}\right) - \right. \\ -Y\left[\dfrac{1+sign(p_m-p_2)}{2}\dfrac{p_m\sqrt{T_m}}{F_2}\varphi\left(\dfrac{p_2}{p_m}\right) - \right. \\ \left.\left. -\dfrac{1+sign(p_2-p_m)}{2}\dfrac{p_2\sqrt{T_2}}{F_2}\varphi\left(\dfrac{p_m}{p_2}\right)\right]\right\} + \\ +\dfrac{k\cdot p_2}{L+x_{02}-x}\dfrac{dx}{dt}; \qquad (2) \\[2mm] \dfrac{dT_2}{dt} = \dfrac{T_2}{p_2}\cdot\dfrac{dp_2}{dt} - \dfrac{T_2}{L+x_{02}-x}\cdot\dfrac{dx}{dt} + \\ +\dfrac{f_2^e\sqrt{k\cdot R}}{F_2\cdot(L+x_{02}-x)}\cdot\left\{(1-Y)\sqrt{T_2}\cdot T_2\cdot\varphi\left(\dfrac{p_a}{p_m}\right) - \right. \\ -Y\left[\dfrac{1+sign(p_m-p_2)}{2}\dfrac{T_2^2\cdot p_m\sqrt{T_m}}{p_2\cdot T_m}\cdot\varphi\left(\dfrac{p_2}{p_m}\right) - \right. \\ \left.\left. -\dfrac{1+sign(p_2-p_m)}{2}\sqrt{T_2}\cdot T_2\cdot\varphi\left(\dfrac{p_m}{p_2}\right)\right]\right\}; \\[2mm] \dfrac{dx}{dt} = v; \\[2mm] \dfrac{dv}{dt} = \dfrac{1}{m}\cdot(p_1\cdot F_1 - p_2\cdot F_2 - P), \end{cases}$$

where k – adiabatic index, $k = 1,4$; $f_1^e = 14\cdot10^{-6}$ m^2; $f_2^e = 13\cdot10^{-6}$ m^2 – effective area of the nominal passage of the inlet and exhaust lines, respectively; R – gas constant, $R = 288$ J/(kg·deg); T_m – air temperature in the main line, $T_m = 393$ °K = 20 °C; F_1 – piston area, $F_1 = 0,00785$ m^2; F_2 – rod cavity area, $F_2 = 0,00659$ m^2; p_m – main line pressure, $p_m =$ =0,6 MPa; x_{01}, x_{02} – initial coordinates of the piston, $x_{01} = x_{02} = 0,01$ m; L – piston stroke, $L = 0,4$ m; m – weight of moving masses (reduced to the piston axis of inertia) $m = 350$ kg; P – static unidirectional (constant-sign) load on the piston, $P = 700$ N; $p_a = 0,1$ MPa – atmospheric pressure.

As an example, let us consider a pneumatic system (Fig. 1) consisting of a double-acting pneumatic cylinder controlled by a monostable 4/2 distributor R and which is one of the most common designs in modern industry. Such a system is controlled by an industrial microcontroller, which, depending on the piston movement phase (acceleration, braking or positioning), changes the value of the distributor control signal Y. Physically, this is implemented by using magnetic sensors located on the cylinder or limit switches that track the piston reaching a certain switching coordinate and, upon reaching it, change the value of the Boolean variable of the distributor control signal. The control map is shown in Fig. 1, where the electrical control signals take the values 1 (current supplied) and 0 (current absent). The calculation scheme for this pneumatic system is shown in Fig. 2.

In order to assess the quality of the pneumatic system, we will calculate its transient process using the mathematical model (2) using the Runge-Kutta numerical method of the 4th order of accuracy with an integration step $1\cdot10^{-3}$ relative to the following variables: p_1 – pressure in the piston cavity; p_2 – pressure in the rod cavity; T_1, T_2 – temperature in the corresponding cylinder cavity; x – current piston coordinate; v – piston speed. Piston braking occurs on a path segment of $L \in (355, 385)$ mm.

The following initial operating conditions of the system were determined during the modeling: at the moment the piston moves from its place $x = x_{01} = 0,01$ m; $v = 0$; $p_1 = 0,1$ MPa; $p_2 = 0,6$ MPa; $T_1 = 293$ K; $T_2 = 293$ K.
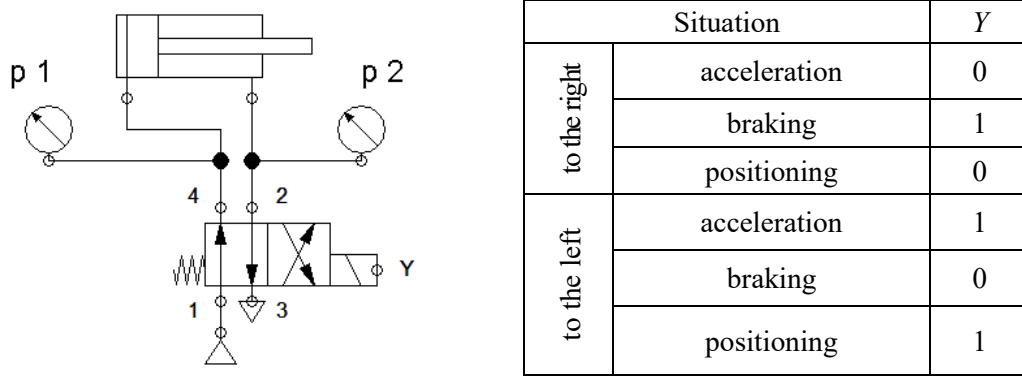
Fig. 1. Diagram of the pneumatic system and the control map of directional valves enabling energy-saving operation mode: Y **– Boolean variable,** $Y = \begin{cases} 1 \\ 0 \end{cases}$.
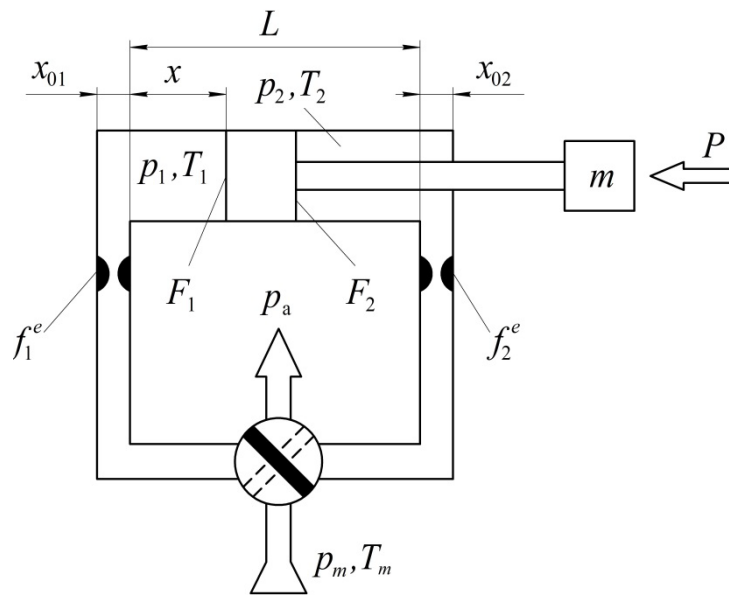

Fig. 2. Computational scheme of the pneumatic system.

Final conditions of the PS operation (at the moment of piston stop): $x = L - x_{01} = 0,4 - 0,01 = 0,39$ m; $v = 0$.

RESEARCH RESULTS AND THEIR DISCUSSION

The calculation results for the system's baseline parameters (curves labeled "1") are presented in Figures 3–5.

From Figure 3, it can be observed that the pressure in the piston (working) chamber rises rapidly and then slightly decreases during acceleration. The piston then continues to move with a constant minimal pressure differential until the onset of braking.

At approximately 1.15 seconds, an electric control signal Y is sent to the braking directional valve (Fig. 1). As a result, compressed air is supplied to the rod chamber from the supply line, while the piston chamber is connected to the atmosphere. This leads to a sharp increase in pressure in the rod chamber and a slight drop in the piston chamber (Fig. 4). When the control signal Y to the braking valve returns to zero, the piston chamber is reconnected to the supply line, leading to a rapid pressure rise p_1 in that chamber and a sharp drop pressure in the rod chamber p_2.

These pressure changes result in rapid temperature fluctuations in the cylinder chambers (Fig. 4), caused by intense air compression and expansion. At the same time, there are short-term significant temperature spikes in the chambers during the braking process. Such temperature swings negatively affect the energy carrier's performance and
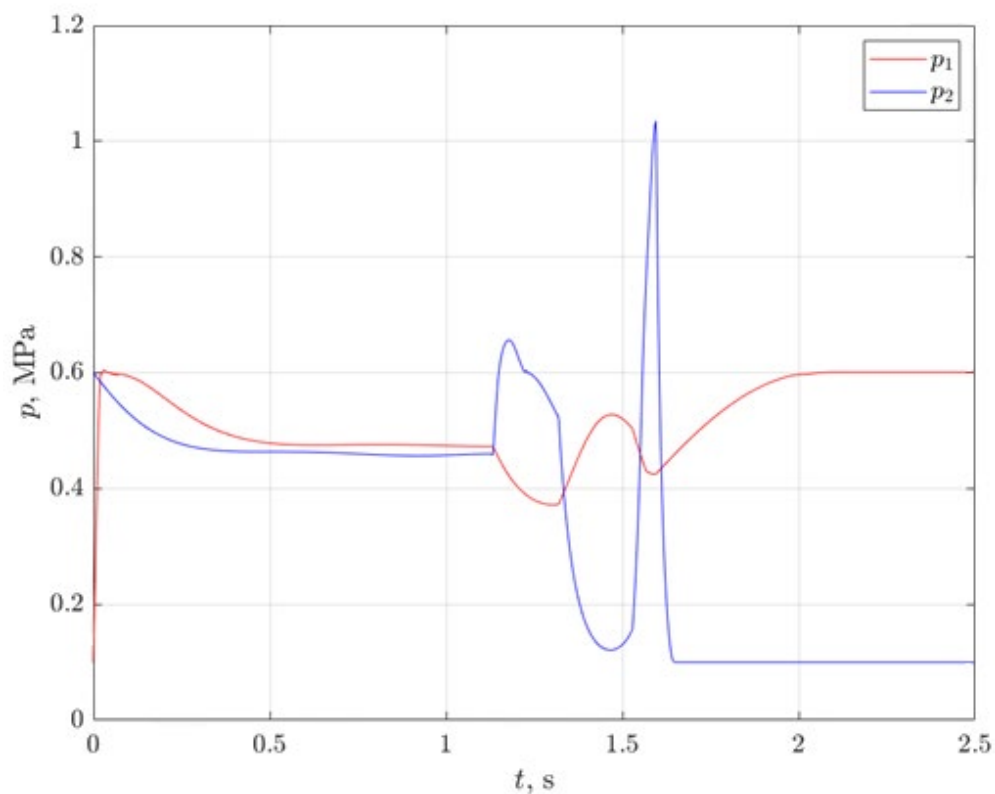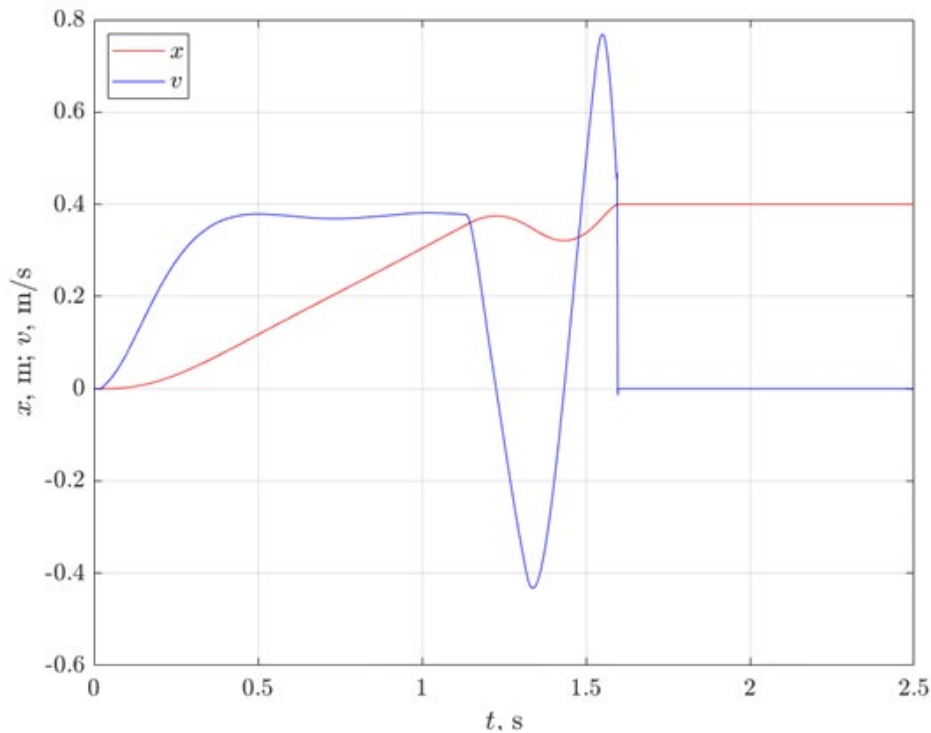
1 – baseline process; 2 – process with optimized braking coordinates
Fig. 3. Transient pressure characteristics in the piston chamber (red line) and rod chamber (blue line) of the cylinder during actuation (motion from left to right, corresponding to the scheme in Fig. 1).
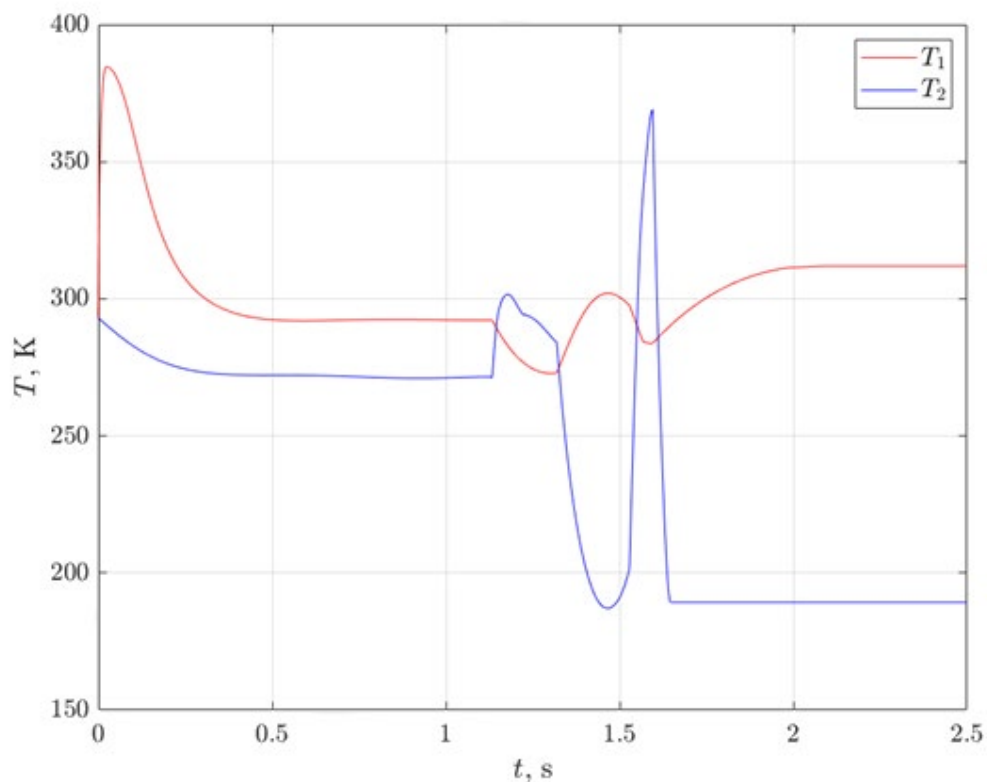
1 – baseline process; 2 – process with optimized braking coordinates
Fig. 4. Transient temperature characteristics in the piston chamber (red line) and rod chamber (blue line) of the cylinder during actuation.

1 – baseline process; 2 – process with optimized braking coordinates
Fig. 5. Transient characteristics of piston velocity (blue line) and displacement (red line) during actuation.

control system accuracy, as prolonged cyclic operation causes metallic components to accumulate heat effects, which in turn influence the temperature of the compressed air in both working and exhaust chambers.

Figure 5 shows the piston displacement and velocity over time. It can be observed that due to the sudden pressure increase in the rod chamber during braking, the piston moves backward over part of the stroke, covering approximately 60 mm in reverse. This significantly reduces the actuator's energy efficiency.

The advantages of this transient process include system stability, satisfactory responsiveness (the transient lasts around 1.65 seconds), and smooth piston acceleration. However, the final piston velocity reaches approximately 0.5 m/s, which results in an impact against the cylinder cap. To avoid this, damping devices are required, but they reduce system energy efficiency due to the release of compressed air into the atmosphere.

To improve the energy efficiency of the system, the working process was optimized. The goal of this optimization was to minimize the piston velocity at the end of the stroke [33]. This required identifying the optimal braking start (x_1) and end (x_2) coordinates that result in minimal final velocity, eliminating impact and

the need for damping devices – thus avoiding additional compressed air losses.

The optimization method chosen for this study was the Nelder – Mead algorithm for multivariable functions (also known as the simplex method), which was implemented in a MATLAB program for simulating transient characteristics of the pneumatic system under optimized parameters.

The simulation results for the system with optimized parameters (curves labeled "2") are shown in Figures 3–5.

As a result of the calculation, the optimal braking start coordinate was determined to be $x_1 = 325$ mm, and the braking end coordinate to be $x_2 = 373$ mm (curve 2 in Fig. 5).

From Figures 3–5, it can be seen that the obtained transient processes for the optimal braking coordinates (curves labeled "2") are similar to the previously calculated ones without optimization (curves labeled "1"). Therefore, the optimized braking start and end coordinates do not fully meet the goal of the optimization: at the final point of the piston trajectory, the velocity is 0.05 m/s (an order of magnitude lower than without optimization – curve 1 in Fig. 5), yet still higher than the required final velocity. Pneumatic rebound is observed (reverse piston movement) over the range from 347 mm to

280 mm (curve 2 in Fig. 5), and the piston moves backward an even greater distance than in the non-optimized case.

To study the effect of specific optimal braking coordinates on the final piston velocity, a MATLAB program was developed to generate a three-dimensional surface plot of the relationship between piston velocity and braking coordinates (Fig. 6). On the graph, the vertical axis represents the piston velocity (m/s); the horizontal axis on the bottom right shows the coordinate where braking begins (m), and the horizontal axis on the left shows the coordinate where braking ends (m).

From Fig. 6, the surface can be conditionally divided into three zones:

– Zone 1 (orange): where the final piston velocity is at its maximum. This occurs when both the start and end of braking happen early (see Table 1);

– Zone 2 (light green): where the final velocity is lower than in Zone 1, but still remains unacceptably high;

– Zone 3 (light blue): where the final velocity approaches an acceptable level (closer to blue), allowing the pneumatic cylinder to operate without the use of a damping device.

According to Table 1, the lowest final piston velocity is achieved when braking starts within the last 10% of the stroke and ends approximately within the final 5%.
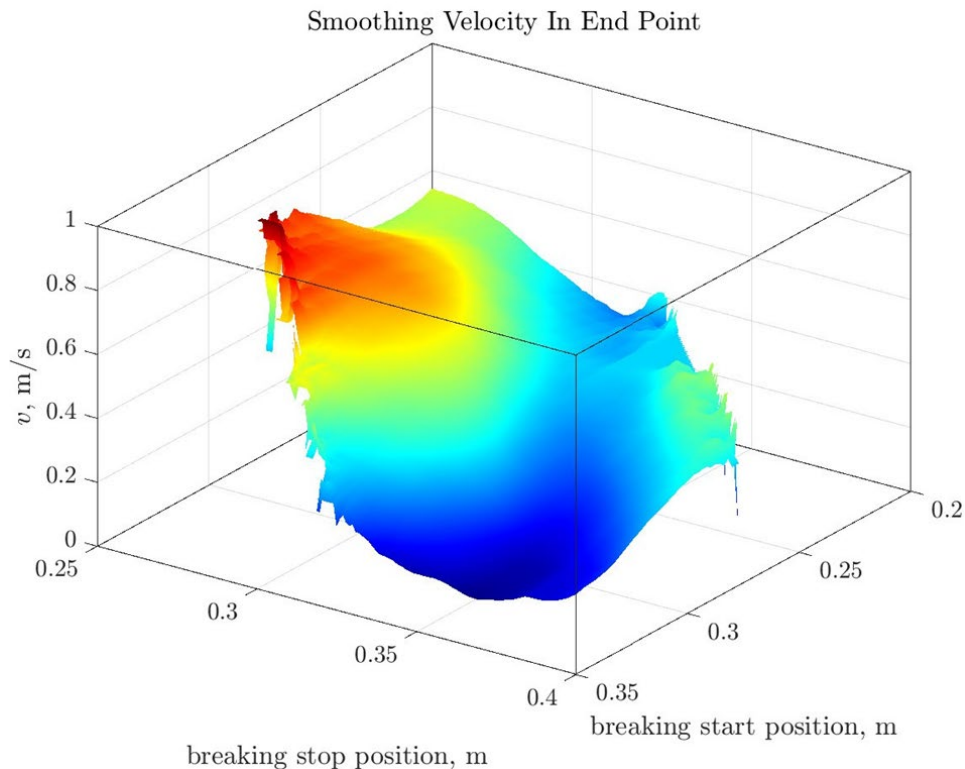

Fig. 6. Surface plot of the relationship between braking path coordinates and piston velocity.

Table 1. Analysis of the effect of braking coordinates on the final cylinder velocity.

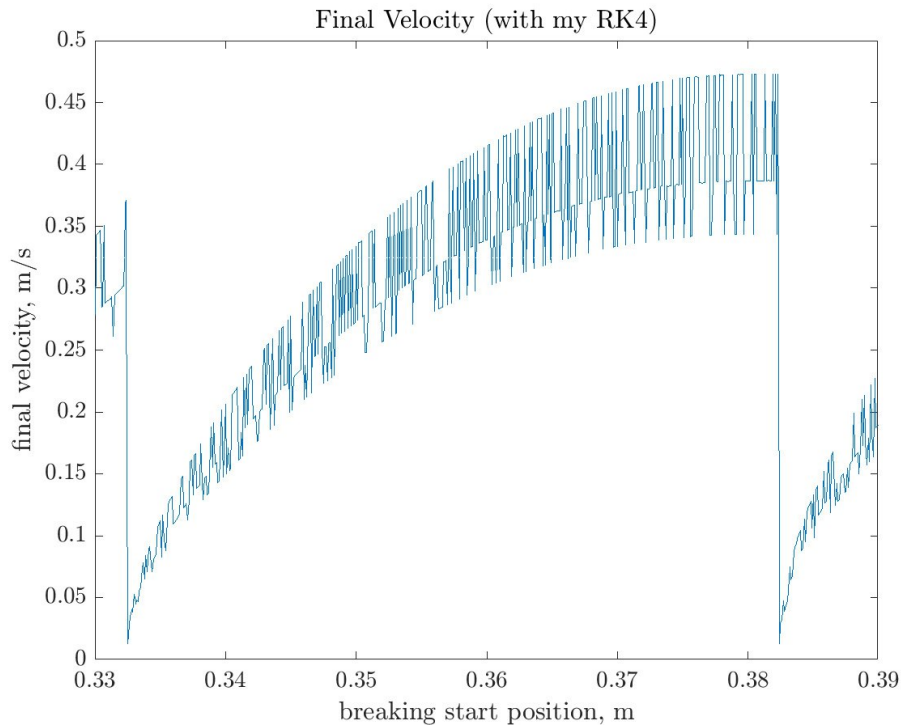| Zone on the graph	Range of the ratio of the braking start coordinate to the overall trajectory of movement, %	The range of the ratio of the coordinates of the end of braking to the general trajectory of movement, %	Range of values of final piston speed, m/s
	52,5 – 79	62,5 – 80	0,5 – 0,9
	56 – 80	70 – 90	0,35 – 0,5
	58 – 85	72,5 – 97,5	0,2 – 0,35
	60 – 92,5	88,5 – 98,5	0,01 – 0,2

Fig. 7. The relationship between the coordinate of the start of braking and the final piston velocity, obtained by integrating the mathematical model using the Runge-Kutta method with a constant step.

At the same time, the shape of the surface (Fig. 6) indicates the absence of a single global extremum, thus ruling out the use of conventional optimization methods such as the Nelder–Mead algorithm, which typically seek a well-defined minimum or maximum.

The objective of this study is to determine the coordinates of a pneumatic actuator that ensure the reduction of piston velocity to a minimum without the use of damping devices, by identifying the start and end coordinates of braking. In its mathematical formulation, this problem belongs to the class of feedback control problems.

To solve such problems, various modern methods related to optimal control with fixed endpoints are used. For example, in [34], implicit endpoint reduction is achieved through approximation: the approach formalizes the transformation of a variable-endpoint problem (stopping constraints) into a fixed-endpoint problem, enabling the application of standard optimal control methods via successive approximation.

In article [35], a theoretical justification is provided for an approach that avoids the direct imposition of strict terminal boundary conditions by introducing penalties in the objective function. This method is applicable for fixed-endpoint control in linear systems and, locally, in nonlinear systems.

Article [36] proposes a method for implementing space and time constraints using a QP (quadratic programming) algorithm, which ensures that the system transitions from a fixed initial state to a specified terminal state within a limited time.

Study [37] explores a numerical optimization method with control and time-scale parameterization, which enables the transformation of variable-endpoint problems into fixed-time problems using additional decision variables.

The method presented in [38] addresses problems with state constraints, but it can be adapted to fixed-endpoint problems. A "tree-based" numerical method is proposed for solving the optimization problem.

To find the optimal braking coordinates – those that result in the minimum final piston velocity – we use an interior-point nonlinear programming algorithm. This is a hybrid method combining two classical optimization approaches: direct search and trust region steps, as described in [39]. The optimization algorithm is implemented in MATLAB.

We assume that the braking end coordinate approaches the final coordinate of the piston's

travel path (where velocity should be zero or nearly zero) exponentially. This reduces the search space to a single variable: the braking start coordinate, which must correspond to the condition of minimizing the final piston velocity.

To implement this algorithm, a MATLAB program was developed to calculate the relationship between the braking start coordinate and the final piston velocity. The program uses the Runge–Kutta method with a fixed integration step (Fig. 7). From the generated graph, the optimal braking start coordinate was determined (for a cylinder stroke of $L = 400$ mm) to be 382 mm.

The resulting transient characteristics of the pneumatic system with optimized (by value iteration) braking coordinates are presented in Figures 8–10. The calculated system parameters are identical to those mentioned above. The results are applicable to systems with significant inertial loads (in the example, the equivalent mass referred to the piston axis is $m = 350$ kg) and a substantial static load acting on the piston (in the example $P = 700$ N).

The obtained velocity and displacement curves (Fig. 8) show that the piston speed increases smoothly and remains stable until braking begins, after which it rapidly decreases. At the final point of the path, the velocity reaches 0.03 m/s, an acceptable value that eliminates the need for damping devices. No reverse displacement of the piston occurs. The transient process lasts approximately 1.25 seconds.

The pressure and temperature change graphs also meet the optimization goals: At the beginning of the piston's movement, the pressure in the piston chamber rises sharply, reaching the supply line pressure, while the pressure in the rod chamber drops (as the system simulates cyclical operation, the initial pressure levels in the chambers are set based on the final values from the previous cycle). A minimal pressure differential is then established, within the range of 0.46–0.48 MPa.

Based on the obtained results (Fig. 5-8), it can be concluded that correctly selected braking coordinates reduce the final piston speed without using a damper, and therefore without releasing air into the atmosphere. This significantly reduces energy losses, which is confirmed by the study [6], which proves that traditional systems with air release through dampers lose up to 100% of the air accumulated during braking. Conversely, the method of changing switching situations allows compressed air to be retained in the system, preserving potential energy.
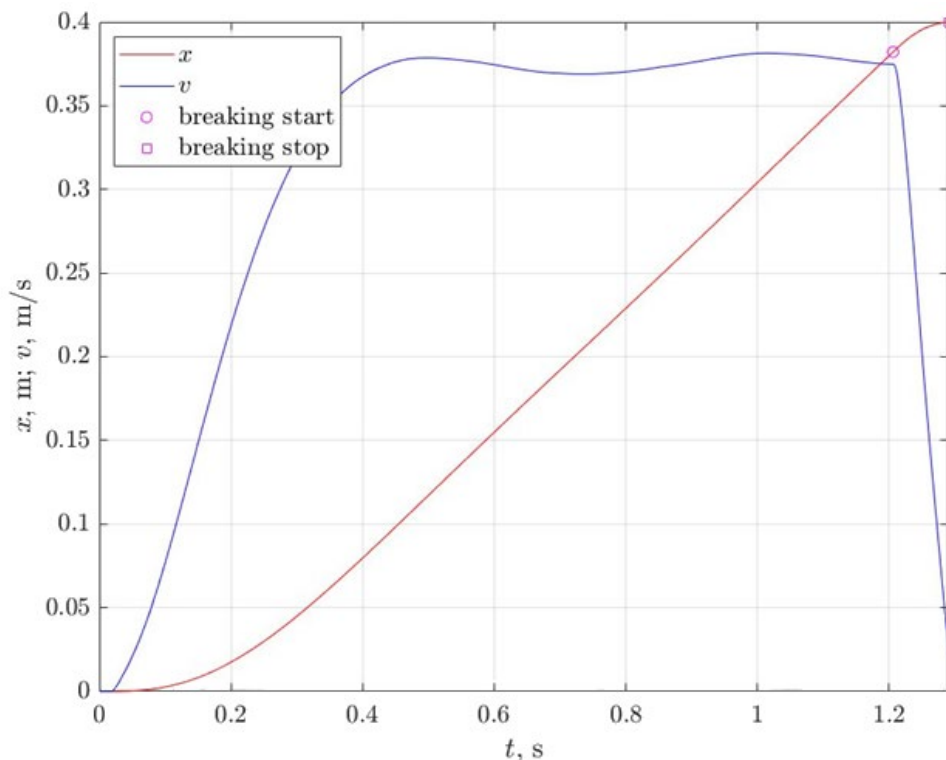

Fig. 8. Transient characteristics of piston velocity (blue line) and displacement (red line) during actuation (determination of braking start coordinate using iterative method).
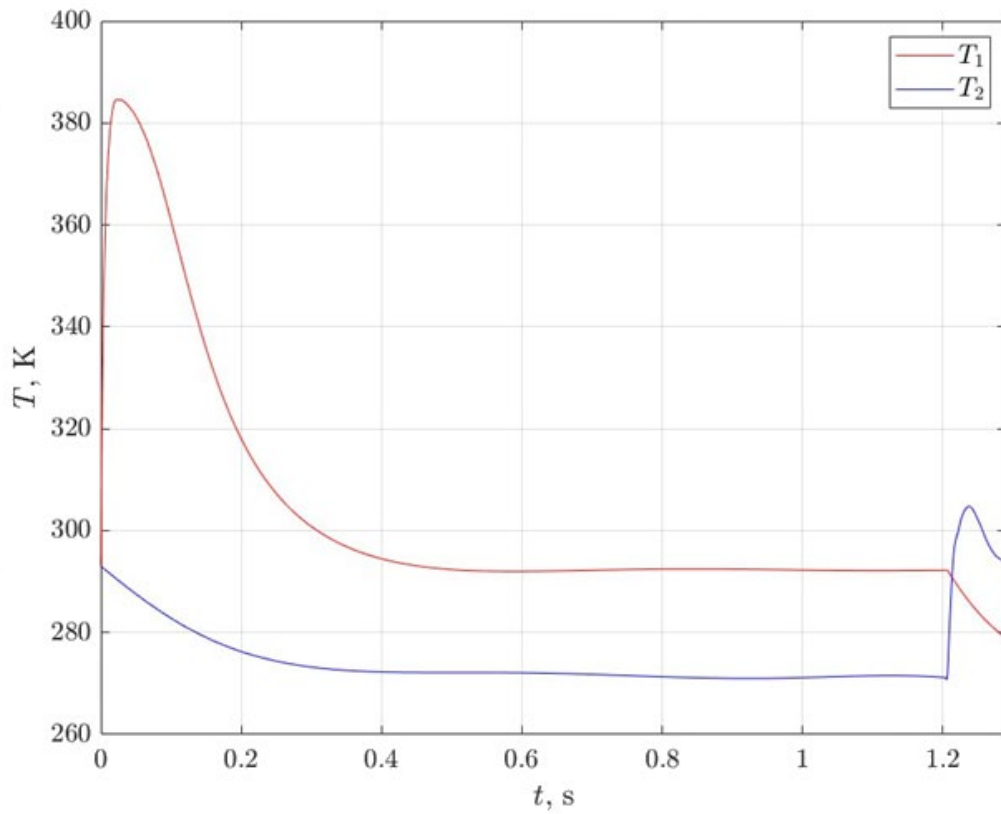
Fig. 9. Transient characteristics for temperature in the piston (red line) and rod (blue line) chambers of the cylinder during actuation (determination of braking start coordinate using iterative method).
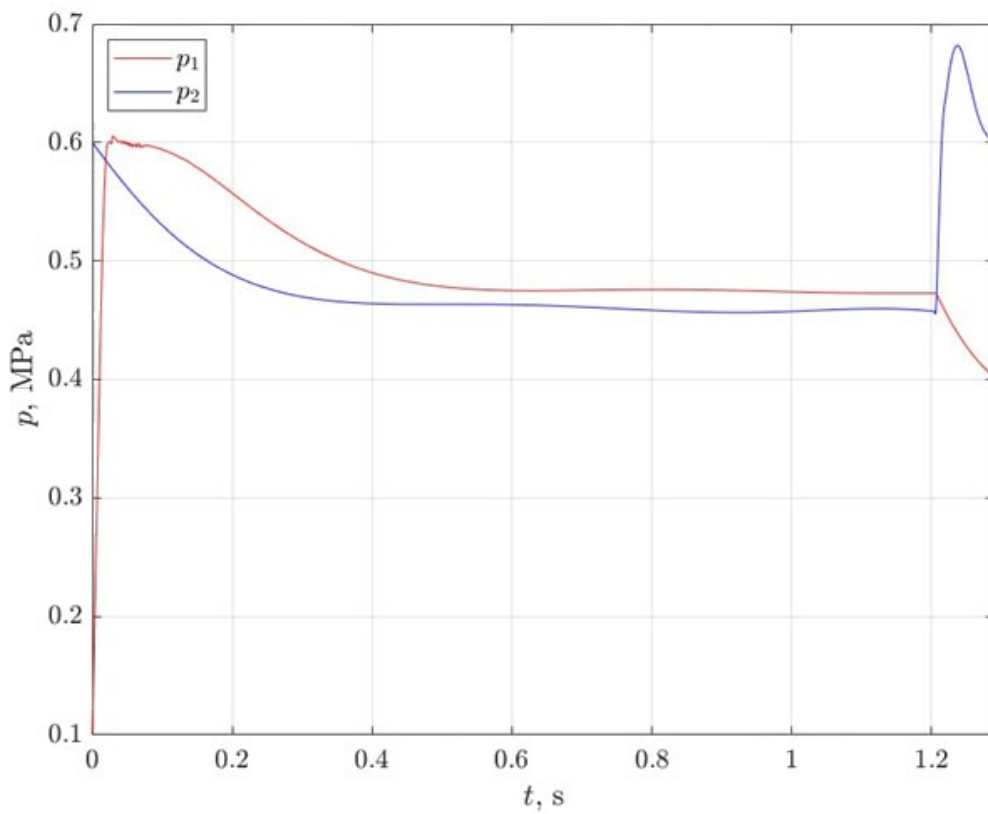

Fig. 10. Transient pressure characteristics in the piston (red line) and rod (blue line) chambers of the cylinder during actuation (determination of braking start coordinate using iterative method).
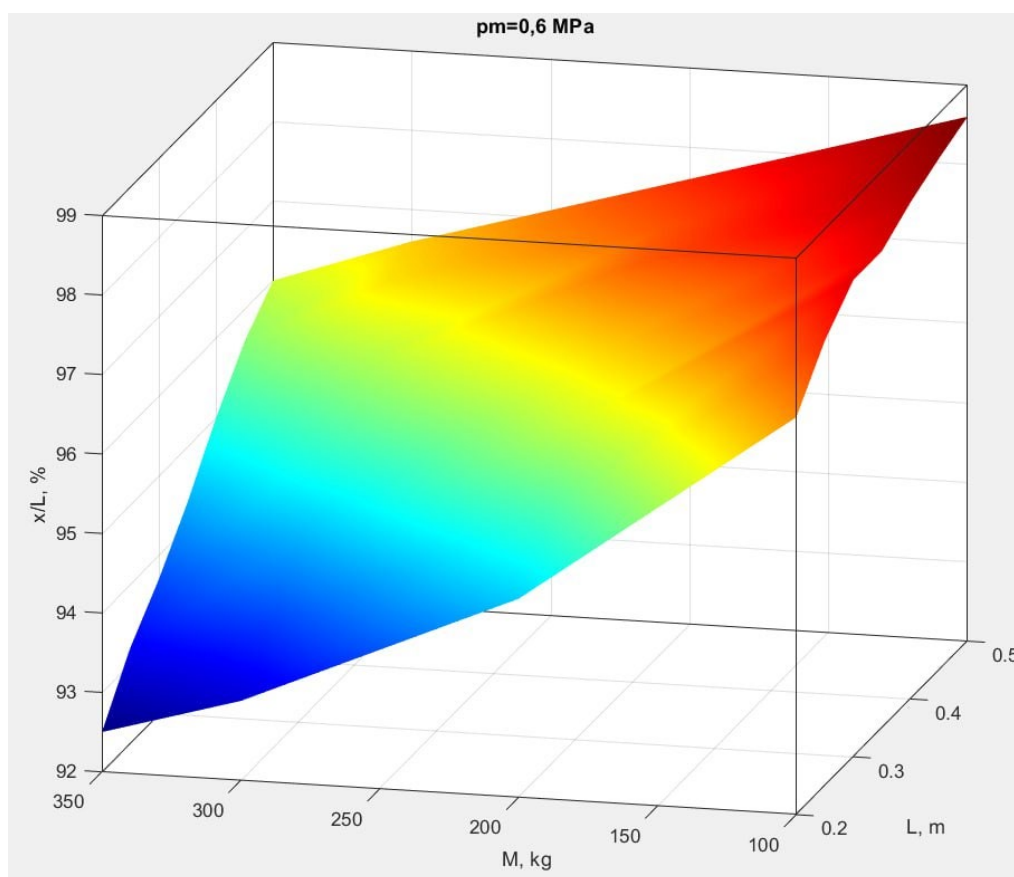
Fig. 11. Surface of the ratio of the coordinate of the start of braking to the length of the piston trajectory, calculated for the ranges of trajectory values ($L = 200...500$ mm), masses of the moving parts of the drive, reduced to the axis of inertia of the cylinder ($m = 100...350$ kg) at the pressure level in the line

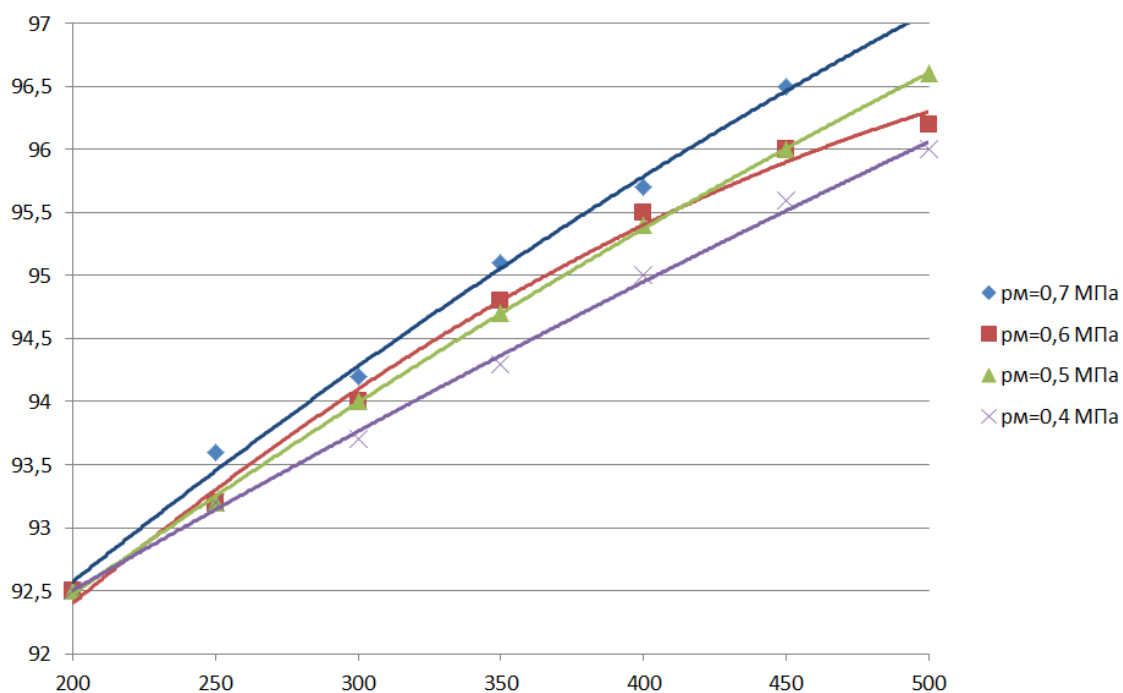$$p_{\text{м}} = 0,6 \cdot 10^{-6} \text{ MPa.}$$

Fig. 12. Percentage ratio of the braking start coordinate to the length of the piston movement trajectory for different supply pressure levels in the pneumatic system.
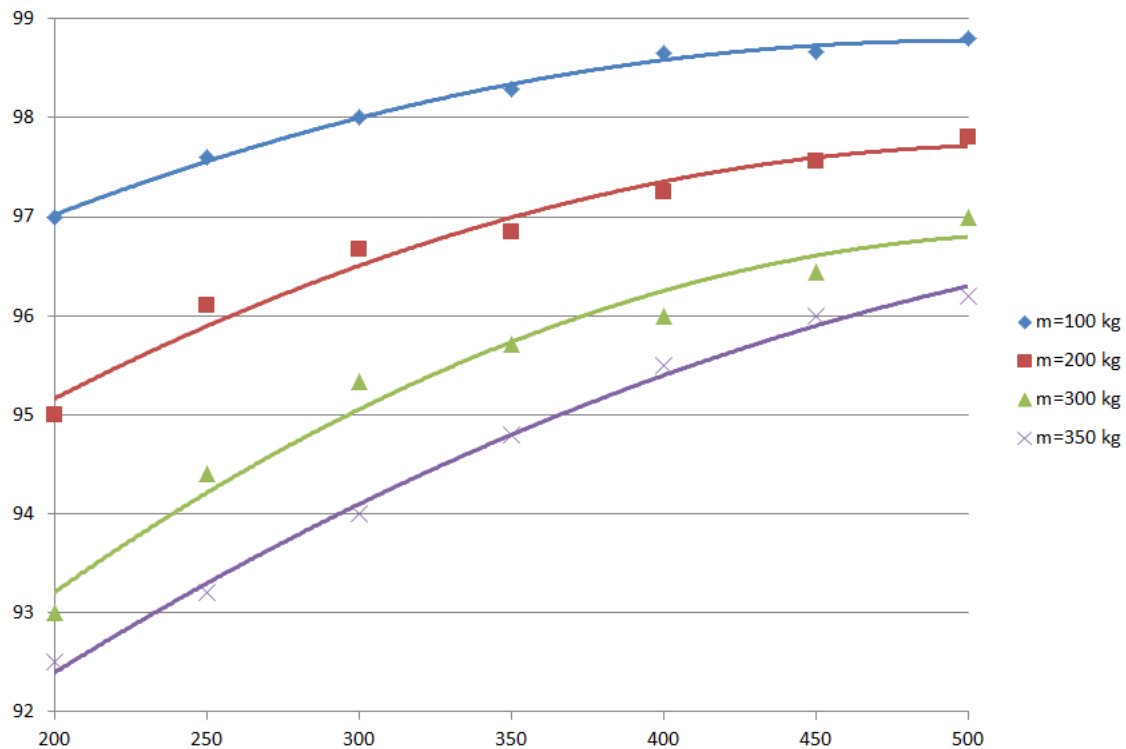
Fig. 13. Percentage ratio of the braking start coordinate to the length of the piston movement trajectory for different values of the mass of the moving parts of the pneumatic drive.

The study [7] confirms that modes with gas expansion (which are implemented similarly to modes with changing switching situations, without air discharge) provide an increase in specific work, and therefore an increase in the efficiency of the pneumatic cylinder by 50-85% compared to traditional methods.

For the studied pneumatic system, based on the developed methodology and calculation program, the analysis of the braking process was carried out for various lengths of the cylinder trajectories ($L = 200...500$ mm) and the values of the masses of the moving parts of the drive, reduced to the axis of inertia of the cylinder ($m = 100...350$ kg), and the behavior of the system at various pressure levels in the supply line in the range of $p_{\text{M}} = 0,4...0,7 \cdot 10^{-6}$ MPa was analyzed (Fig. 11). Normalized values of the ratio of the coordinate of the beginning of braking to the length of the path that the piston passes (Fig. 12) and to the mass of the moving parts of the drive (Fig. 13) were found. The proposed methodology allows to select the coordinate of the beginning of braking at the stage of designing a pneumatic system without preliminary calculations, simplifying the process of synthesis of energy-saving solutions in a pneumatic drive.

The calculation results indicate a relationship between the braking start point, the mass of the moving parts of the drive and the length of the the cylinder's travel path, while the pressure in the supply line in the calculated range of $p_{\text{M}} = 0,4...0,7 \cdot 10^{-6}$ MPa has an insignificant effect on the start time of braking: the surfaces of the ratio of the parameters under study differ from each other by less than 5%, therefore, Fig. 11 shows the surface for the $p_{\text{M}} = 0,6 \cdot 10^{-6}$ MPa value. The longer the travel path, the closer the braking starts to the end of the stroke. However, within the studied range, the braking always begins within the final 7.5% of the piston stroke length. Increasing the supply line pressure shifts the breaking point even closer to the end of the travel path. The greatest effect on the start time of breaking is exerted by the mass of the moving parts of the drive (Fig. 13): the higher it is, the smaller will be the ratio of the braking coordinate and the length of the path traveled by the piston.

CONCLUSIONS

As a result of the optimization studies, the best outcome was achieved using the method of iterative value selection, where braking occurs closer to the end point of the piston's travel path.

In this case, a final piston velocity close to zero was attained – 0.03 m/s. Consequently, such a pneumatic system does not require damping devices to reduce the piston's speed at the end of the stroke or the release of compressed air into the atmosphere, thereby ensuring an energy-efficient mode of actuator operation.

The obtained results allow for the selection of the supply pressure, design parameters, equipment sizing, and adjustment settings during the design phase of the pneumatic system in a way that ensures a transient process without pneumatic rebound and with a final piston velocity close to zero. As a result, the overall efficiency significantly increases, since the energy-saving mode of the pneumatic system is achieved by eliminating the discharge of compressed air into the atmosphere during the deceleration process.

REFERENCES

[1] Statista Research Department. (2025). *Verteilung des Stromverbrauchs in Deutschland nach Verbrauchergruppen in den Jahren 2014 und 2024*. Statista. Retrieved from https://de.statista.com/statistik/daten/studie/236757/umfrage/stromverbrauch-nach-sektoren-in-deutschland/ (Accessed: 13.06.2025).

[2] Radgen, P., & Blaustein, E. (2001). *Compressed Air Systems in the European Union: Energy, Emissions, Savings Potential and Policy Actions*. Stuttgart: Fraunhofer Institute for Systems Technology and Innovation. https://publica.fraunhofer.de/entities/publication/60fbadfb-caf9-4e21-bd6e-5095fbff1964 (Accessed: 13.06.2025).

[3] Radermacher, T., Merx, M., Sitte, A., Boyko, V., & Unger, M. (2021). *Potenzialstudie Energie-/Kosteneinsparung in der Fluidtechnik: Final report No. 37EV181030*. TU Dresden, University of Stuttgart. https://www.umweltbundesamt.de/publikationen/potenzialstudie-energie-kosteneinsparung-in-der (Accessed: 13.06.2025).

[4] Šešlija, D. D., Milenković, I. M., Dudić, S. P., & Šulc, J. I. (2016). Improving energy efficiency in compressed air systems – Practical experiences. *Thermal Science*. Article 20(00):22-22. DOI:10.2298/TSCI151110022S

[5] Festo AG & Co. KG (2012). Energy Efficiency in Production in the Drive and Handling Technology Field (EnEffAH). Final Report No. 0327484A-E. https://www.eneffah.de/EnEffAH_Broschuere_engl.pdf (Accessed: 13.06.2025).

[6] Dindor, R. (2012). Estimating Potential Energy Savings in Compressed Air Systems. *Procedia Engineering*, 39, 204–211. https://doi.org/10.1016/j.proeng.2012.07.026

[7] Gailis M., Rudzitis, J., Madissoo, M., and Kreicbergs J. (2020). Research on energy efficiency of pneumatic cylinder for pneumatic vehicle motor. *Agronomy Research*, 18(S1), 823–841. https://doi.org/10.15159/AR.20.048

[8] McKane, A., Hasanbeigi, A. (2011). Motor systems energy efficiency supply curves: A methodology for assessing the energy efficiency potential of industrial motor systems. *Energy Policy*, 39, Issue 10. https://doi.org/10.1016/j.enpol.2011.08.004

[9] Rihong, X., Qungui, L., & Kai, X. (2022). Dynamic simulation and optimization of cushioning performance in high-speed pneumatic cylinders. Processes, 10(4), 819. DOI: https://doi.org/10.3390/pr10040819

[10] Andrenko, P., Hrechka, I., Khovanskyi, S., Rogovyi, A., & Svynarenko, M. (2021). Improving the technical level of hydraulic machines, hydraulic units and hydraulic devices using a definitive assessment criterion at the design stage. Journal of Mechanical Engineering (JMechE), 18(3): 57-76. DOI:10.24191/jmeche.v18i3.15414

[11] Dvořák L., Fuksa L., Ledvoň M., Brzezina P. (2019). Experimental Verification of Pneumatic Cylinder External Pneumatic Cushioning. *EPJ Web of Conferences*, Vol. 213, Article 02015. DOI:10.1051/epjconf/201921302015

[12] Nazarov, F., Weber, J. (2021) Modelling, Simulation and Validation of the Pneumatic End-Position Cylinder Cushioning. *Proceedings of the 17th Scandinavian International Conference on Fluid Power (SICFP'21)*. May 31 – June 2, 2021. – Linköping University Electronic Press, 206–210. https://ecp.ep.liu.se/index.php/sims/article/view/131

[13] Rihong Z., Qungui D. (2016). Dynamic Simulation and Optimization of Cushioning Performance in High Speed Pneumatic Cylinders. *International Journal of*

Simulation: Systems, Science & Technology. Article 17(17):17.1-17.6. DOI: 10.5013/IJSSST.a.17.17.17

[14] Panchenko A., Voloshina A., Panchenko I. at all (2021). Influence of the Shape of Windows on the Throughput of the Planetary Hydraulic Motor's Distribution System. *Advances in Design, Simulation and Manufacturing IV. DSMIE 2021. Lecture Notes in Mechanical Engineering*. Cham: Springer, Vol. 2, 146–155. https://doi.org/10.1007/978-3-030-77823-1_15

[15] Panchenko A., Voloshina A., Sadullozoda S.S. at all (2022). The Changes in the Output Parameters of Planetary Hydraulic Machines with the Increase in the Gap Between Their Rotors. *Advanced Manufacturing Processes IV. InterPartner 2022. Lecture Notes in Mechanical Engineering*. Cham: Springer, 540–551. https://doi.org/10.1007/978-3-031-16651-8_51

[16] Yu, Q., Jianwei, Z., Qiancheng, W., Xuxiao, Z. (2021) Experimental Study of a New Pneumatic Actuating System Using Exhaust Recycling. *Sustainability*, *13*(4), 1645. https://doi.org/10.3390/su13041645

[17] Boyko, V., Weber, J. Energy Efficiency of Pneumatic Actuating Systems with Pressure-Based Air Supply Cut-Off. *Actuators,* 13(1), 44. https://doi.org/10.3390/act13010044

[18] Gryboś, D, Leszczyński, J. S. (2024) A Review of Energy Overconsumption Reduction Methods in the Utilization Stage in Compressed Air Systems. *Energies*, *17*(6), 1495. https://doi.org/10.3390/en17061495

[19] Krutikov, G., Stryzhak, M. (2025). Assessment of the Influence of Design Parameters of a Pneumatic Drive on the Energy Efficiency of the Working Process. *Problems of the Regional Energetics*, 2-66, 190 – 204. DOI: 10.52254/1857-0070.2025.2-66.16

[20] Hua-Shu, D., Gang, J. (2016) Numerical simulation of flow instability and heat transfer of natural convection in a differentially heated cavity. International Journal of Heat and Mass Transfer, 103, 370-381. https://doi.org/10.1016/j.ijheatmasstransfer.2016.07.039

[21] Borri, E., Tafone, A., Comodi, G. at all (2022). Compressed Air Energy Storage – An Overview of Research Trends and Gaps through a Bibliometric Analysis. *Energies*, 15(20), 7692. https://doi.org/10.3390/en15207692

[22] Shi, Y., Cai, M., Xu, W. et all (2019). Methods to Evaluate and Measure Power of Pneumatic System and Their Applications. *Chinese Journal of Mechanical Engineering*, 32, Article 42. https://doi.org/10.1186/s10033-019-0354-6

[23] Jiménez, M., Kurmyshev, E., Castañeda, C. (2020). Experimental Study of Double-Acting Pneumatic Cylinder. *Experimental Techniques*, 44(2). DOI: 10.1007/s40799-020-00359-8

[24] Mare, J.-C., Geider, O., Colin, S. (2020). An Improved Dynamic Model of Pneumatic Actuators. *International Journal of Fluid Power*, 1(2), 39–49. DOI:10.1080/14399776.2000.10781090

[25] Roos, P., Haselbacher, A. (2022). Analytical modeling of advanced adiabatic compressed air energy storage: Literature review and new models. Renewable & Sustainable Energy Reviews, 163, 112464. https://doi.org/10.1016/j.rser.2022.112464

[26] Lemmon, E. W., Huber, M. L., McLinden, M. O. (2013). NIST Reference Fluid Thermodynamic and Transport Properties – REFPROP, Version 9.1. *U.S. Department of Commerce, National Institute of Standards and Technology*, 190 p.

[27] Vestfálová, M., Šafařík, P. (2019). Determination of the applicability limits of the ideal gas model for the calculation of moist air properties. *The European Physical Journal Conferences*, 180(3), 02115. DOI:10.1051/epjconf/201818002115

[28] Hertz, O. V. & Kreinin, G. V. (1975). *Design of pneumatic drives.* Moscow: Mashinobuduvannya, 272 pp.

[29] Hertz, O. W. (1985). *Dynamics of pneumatic systems of machines*. Moscow: Mashinobuduvannya, 256 pp.

[30] Matsukawa, Y., & Tsukahara, T. (2025). Transition between supercritical and subcritical turbulent states in Taylor–Couette–Poiseuille flow. *International Journal of Heat and Fluid Flow*, *101*, 109667. DOI: 10.1016/j.ijheatfluidflow.2024.109667

[31] Liu, J., Xiao, Y., Li, M., Tao, J., & Xu, S. (2020). Intermittency, moments and friction coefficient during subcritical transition in channel flow. *Entropy*, *22*(12), 1399. DOI: 10.3390/e22121399

[32] Kamiński, Z. (2011). Mathematical Modeling of Pneumatic Pipes in a Simulation of Heterogeneous Engineering Systems. Journal of Fluids Engineering, 133(12):121401. DOI:10.1115/1.4005261

[33] Romasevych Yu, Loveikin V., and Makarets V. (2022). PID-controller tuning algorithm development for a dynamical system «crane-load». Machinery & Energetics, 13(4): 72–80. https://doi.org/10.31548/machenergy.13(4).2022.72-80

[34] Lin, Q., Loxton, R., Teo, K.L., Wu, Y.H. (2015). Optimal control problems with stopping constraints. *Journal of Global Optimization*, Vol. 63, 835–861. DOI: 10.1007/s10898-015-0286-3

[35] Dolgopolik, M.V. Exact penalty functions for optimal control problems II: Exact penalisation of terminal and pointwise state constraints (2020). *Optimal Control Applications and Methods*. Vol. 41, Iss. 3, 898–947. DOI: 10.1002/oca.2577

[36] Garg K., Shah P., Lamperski A., Arcak M. Fixed-Time Control under Spatiotemporal and Input Constraints: a Quadratic Programming based approach (2022). *Automatica*. Vol. 141: 110314. https://doi.org/10.1016/j.automatica.2022.110314

[37] Wang Y., Yu C., Teo K. L. A new computational strategy for optimal control problem with a cost on changing control (2016). *Numerical Algebra, Control and Optimization*, Vol. 6(3), 339-364. doi: 10.3934/naco.2016016

[38] Alla A., Falcone M., Saluzzi L. A tree structure algorithm for optimal control problems with state constraints (2020). *Rendiconti di Matematica e delle sue Applicazioni*, Vol. 41, No. 3–4, 193–221. DOI: 10.48550/arXiv.2009.12384

[39] Waltz, R. A., Morales, J. L., Nocedal, J. and Orban, D. An interior algorithm for nonlinear optimization that combines line search and trust region steps (2006). *Mathematical Programming*, Vol 107, No. 3, 391–408. DOI: 10.1007/s10107-004-0560-5

Information about authors

Stryzhak Mariana Heorhiyivna
Candidate of Technical Sciences, National Technical University "Kharkiv Polytechnic Institute", Associate Professor of the Department of Machine Parts and Hydropneumatic Systems, Kharkiv, Ukraine
Research interests: modeling and automation of technical systems
mariana.stryzhak@khpi.edu.ua

Rogovyi Andrii Serhiyovych
Doctor of Technical Sciences, Professor, National Technical University "Kharkiv Polytechnic Institute", Head of the Department of Department of Hydraulic Machines named after G.F. Proskura, Kharkiv, Ukraine.
Research interests: inkjet technology; vortex devices; vortex-chamber blowers; swirling currents; computational fluid dynamics
andrii.rogovyi@khpi.edu.ua

Iglin Serhiy Petrovych
Candidate of Technical Sciences, National Technical University "Kharkiv Polytechnic Institute", Associate Professor of the Department Computer Mathematics and Data Analysis, Kharkiv, Ukraine
Research interests: discrete structures and data structures; numerical methods; modern problems of data mining
sergii.iglin@khpi.edu.ua